

# High-Stability Hydrogenated Silicon–Carbon Clusters: A Full Study of $\text{Si}_2\text{C}_2\text{H}_2$ in Comparison to $\text{Si}_2\text{C}_2$ , $\text{C}_2\text{B}_2\text{H}_4$ , and Other Similar Species

Aristides D. Zdetsis

Department of Physics, University of Patras, GR-26500 Patras, Greece

Received: March 5, 2008

The structural and electronic characteristics of the  $\text{Si}_2\text{C}_2\text{H}_2$  and  $\text{Si}_2\text{C}_2$  clusters are studied by ab initio calculations based on coupled cluster and density functional theory using the hybrid B3LYP functional. In addition, similar species, such as  $\text{SiC}_2\text{H}_2$  and  $\text{Si}_3\text{C}_2\text{H}_2$ , are also studied for comparison. It is illustrated that the lowest energy structures of all three hydrogenated clusters, which have the general form  $\text{Si}_n(\text{CH})_2$ ,  $n = 1, 2, 3$ , are fully analogous to the structures of the corresponding organometallic isovalent carboranes. The most stable structure of  $\text{Si}_2\text{C}_2\text{H}_2$  is obtained by attaching two hydrogens onto the carbon atoms of a higher energy (+1.5 eV) planar trapezoidal structure of  $\text{Si}_2\text{C}_2$ , followed by geometry optimization which leads to puckering of the planar structure. Furthermore, it is demonstrated that  $\text{Si}_2\text{C}_2\text{H}_2$  and the other two “similar” hydrogenated clusters are much more stable than the corresponding bare nonhydrogenated clusters. Comparison of  $\text{Si}_2\text{C}_2\text{H}_2$  and  $\text{C}_2\text{B}_2\text{H}_4$  shows that their structural and bonding similarity includes also nuclear rearrangement similarity. The two species are isomerizable with an energy difference between their lowest energy puckered 1,2- and 1,3-isomers of about  $\pm 0.3$  eV. It is suggested that  $\text{SiC}_2\text{H}_2$ ,  $\text{Si}_2\text{C}_2\text{H}_2$ , and  $\text{Si}_3\text{C}_2\text{H}_2$  are special cases of a larger class of stable clusters. It is speculated on the basis of the calculated infrared spectrum that  $\text{Si}_2\text{C}_2\text{H}_2$  and perhaps other members of this class of clusters could be found in appreciable abundance in interstellar space.

## 1. Introduction

The field of mixed silicon–carbon clusters has been active for more than 10 years with numerous experimental and theoretical studies and publications.<sup>1–12</sup> The study of  $\text{Si}_n\text{C}_m$  clusters is very challenging in view of the complexity of the structures and spectroscopies of these clusters. Aside from their importance to the silicon carbide industry, several of these clusters, such as  $\text{SiC}$ ,  $\text{SiC}_2$ , and  $\text{SiC}_4$  (and others) have been identified in circumstellar space,<sup>1,13,14</sup> triggering more spectroscopic studies and theoretical investigations. As a result,  $\text{Si}_n\text{C}_m$  clusters have been (and continue to be) well studied.

However, contrary to hydrogenated Si clusters,<sup>15–17</sup> hydrogenated silicon–carbon clusters have not been studied up to now, although they could be proven at least as important as the bare silicon–carbon clusters. Such hydrogenated clusters, in addition to the role they could play for hydrogenated amorphous silicon–carbide thin films,<sup>18</sup> could be also present in interstellar space as bare  $\text{Si}_n\text{C}_m$  clusters (in view of the large hydrogen abundance) and be responsible for some of the “unidentified” or controversial infrared (IR) lines from stellar atmospheres and circumstellar space.<sup>19–23</sup> These “unidentified” lines have been attributed among others to hydrogenated carbon fullerenes,<sup>19–21</sup> as  $\text{C}_{60}\text{H}_{60}$  and/or higher fullerenes such as  $\text{C}_{180}\text{H}_{180}$  (ref 21). The main feature of the “unassigned” stellar absorption spectrum consists of a plateau in the region of  $2800\text{--}3100\text{ cm}^{-1}$  with several well-defined peaks.<sup>19,21</sup> It is clear that this spectrum is not due to a single source.<sup>19,21</sup> For instance, the astronomical emission at  $3040\text{ cm}^{-1}$ , located at the typical frequency of  $\text{sp}^2$  aromatic C–H stretching, was initially attributed by Webster<sup>19</sup> to partially hydrogenated carbon fullerenes. However, more recently it was considered as more likely to come from either “puckered fullerenes”<sup>20,21</sup> or from fullerenes bombarded by atomic hydrogen,<sup>22</sup> or polycyclic aromatic hydrocarbons.<sup>23</sup> Therefore, this particular peak (at  $3040\text{ cm}^{-1}$ ), which seems to

be of “much different origin”, appears also to be the most controversial. Since, the calculated IR spectra for all three lowest energy structures of  $\text{Si}_2\text{C}_2\text{H}_2$  obtained here contain IR lines in the vicinity of this value, it is reasonable to assume that  $\text{Si}_2\text{C}_2\text{H}_2$ , and other similar species discussed in the present work could be possible sources of that peak. Furthermore, in support of this suggestion, in particular for  $\text{Si}_2\text{C}_2\text{H}_2$ , is the fact that the maximum intensity of the stellar IR spectrum corresponds to the frequency around  $1290\text{ cm}^{-1}$ . As will be seen later the two lowest energy isomers of  $\text{Si}_2\text{C}_2\text{H}_2$  have maximum and second maximum intensities, respectively, in the vicinity of this value. The possibility of identifying  $\text{Si}_2\text{C}_2\text{H}_2$  (and perhaps other similar species) in interstellar medium is very stimulating and challenging for the study of these species.

Furthermore, additional motivation for the study of  $\text{Si}_2\text{C}_2\text{H}_2$  (and other related hydrogenated clusters of the general form  $\text{Si}_n\text{C}_2\text{H}_2$ ,  $n = 1, 2, 3$ ) is the anticipated homology<sup>24,25</sup> with the isovalent carborane  $\text{C}_2\text{B}_2\text{H}_4$ , based on a similar homology<sup>24,25</sup> of  $\text{Si}_n^{2-}$  cluster dianions (and clusters) with the isovalent  $\text{B}_n\text{H}_n^{2-}$  boranes. Such homology, if proven, would be extremely useful for the understanding of structural and bonding properties of these species (and the possible design of hydrogenated silicon–carbon clusters and composite materials with desired properties) taking full advantage of the well-known and well-tested structural (and other) rules and stability criteria developed for boranes and carboranes.<sup>26–30</sup> In addition, depending on the extent of this homology, one could (1) examine several exciting properties from the rich organometallic chemistry (such as isomerization, fluxionality, three-dimensional aromaticity) and (2) obtain the structure of the corresponding bare silicon–carbon clusters in a systematic and well-defined way analogous to the one described in ref 25 for silicon clusters.

In favor of such similarity to boranes and carboranes one could use beforehand some simple structural rules which have been suggested by the author and his collaborators<sup>3–5</sup> for silicon

carbon clusters and tested by many others (see for instance refs 4, 6–8, 11, and 12). These structural rules, which are mainly based on the relative strength of the C–C, Si–C, and Si–Si interactions, and the possibility of multicenter bonding, could be broadly considered as analogous to the well-known structural rules for boranes (and carboranes).<sup>26–30</sup> In fact the aspects of multicenter bonding and alternating charges<sup>3,5</sup> are similar to the multicenter bonding<sup>26,27,29,30</sup> and alternating charges<sup>28</sup> of the deltahedral closo-boranes and carboranes. To verify this homology and structural similarity the isovalent carborane  $C_2B_2H_4$  has been studied in parallel to  $Si_2C_2H_2$ , and similar isovalent pairs have been considered for  $SiC_2H_2$  and  $Si_3C_2H_2$ .

The presentation of the current work is organized as follows: In the next section 2 some technical details of the calculations are briefly discussed, whereas the central results of the calculations for  $Si_2C_2H_2$ ,  $Si_2C_2$ , and  $C_2B_2H_4$  are presented and discussed rather extensively in section 3. The comparison of the structural and bonding properties of  $C_2B_2H_4$  and  $Si_2C_2H_2$ , which is the focus of the present study, is used to establish the (anticipated) structural and electronic similarity of the two species. In section 4 the results of the calculations for  $SiC_2H_2$ ,  $SiC_2$ , and  $C_2BH_3$  are presented and reviewed in order to support the claimed similarity between the  $Si_nC_2H_{n+2}$  clusters and the corresponding “carboranes” for this particular “borderline”  $n = 1$  case. Similarly, the results for  $Si_3C_2H_2$  and  $C_2B_3H_5$  are summarized briefly in section 5 to further reinforce the suggested structural similarity and homology. Finally, the main conclusions and findings of the present work are recapitulated in the last section, 6.

## 2. Technical Details

The calculations for all structures, initial and final geometries, and optimizations, were first performed within density functional theory (DFT), using the hybrid exchange and correlation functional of Becke–Lee, Parr, and Yang (B3LYP).<sup>31</sup> Subsequently, the lower energy structures (including the lowest and higher energy structures up to 2.0 eV above the lowest) were further optimized with the coupled-cluster method, including single and double excitations, in parallel with second-order Moller–Plesset perturbation theory (MP2). The final energies, at the CCSD geometries, were further calculated at the coupled-clusters CCSD(T) level which in addition includes in a perturbative way the triple excitations. All these calculations were performed with the GAUSSIAN program package,<sup>32</sup> using the TZVP, the correlation consistent cc-PVTZ, and 6-311+G(2d, p) basis sets as implemented in this package.<sup>32</sup> The geometry optimizations were run with and without symmetry constraints, and the calculations were supplemented with vibrational frequency calculations to obtain the IR spectrum and check at the same time for imaginary frequencies. First, the lower and higher energy structures of  $Si_2C_2$  were calculated from scratch and/or recalculated on the basis of the literature<sup>1–6,9,10</sup> and by proper substitutions in the structures of  $Si_4$  and  $C_4$ . Similarly, the structures of  $SiC_2$  and  $Si_3C_2$  were (re)calculated from the known results in the literature<sup>1–6</sup> and/or by proper substitutions in the structures of  $C_3$ ,  $C_5$ , and  $Si_5$  or  $Si_5^{2-}$  (see, for instance, ref 25). Then, starting geometries for the geometry optimizations of  $Si_2C_2H_2$  structures were obtained by hydrogenating (in all possible reasonable ways) the structures of the bare  $Si_2C_2$ ,  $SiC_2$ , and  $Si_3C_2$  clusters. Hydrogens were attached either to C or Si atoms or both in all possible and plausible combinations, generating a plethora of hydrogenated clusters which were optimized at the B3LYP/TZVP level (first) without any symmetry constraints. Then, the relatively low energy structures

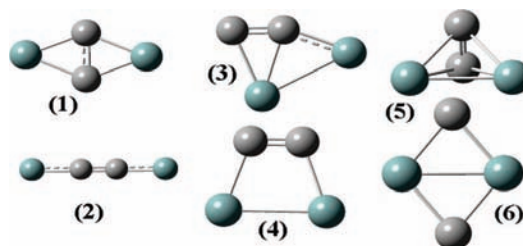


Figure 1. Lower energy optimized structures of  $Si_2C_2$ .

TABLE 1: Total and Relative Energies ( $E/\Delta E$ ) of  $Si_2C_2$  Isomers at the CCSD(T) and B3LYP Levels of Theory Using the 6-311+G(2d,p) Basis Set, Together with Calculated Atomization Energies for the Lowest Energy Structure (in Parentheses) Based on Total Electronic Energies at the B3LYP Level (Zero-Point Energies Are Not Included)<sup>a</sup>

structure/symmetry	B3LYP $E$ (hy)/ $\Delta E$ (eV)	CCSD(T) $E$ (hy)/ $\Delta E$ (eV)
1 $D_{2h} \ ^1A_g$	–655.107977 (11.76)	–653.962288 0
2 $D_{\infty h} \ ^3\Sigma_g$	–0.05	+0.33
3 $C_s \ ^1A'$	+0.22	+0.18
2 $D_{\infty h} \ ^1\Sigma_g$	+0.50	+0.63
4 $C_{2v} \ ^1A_1$	+1.55	+1.56
5 $C_s \ ^1A'$	+2.08	+1.92
6 $D_{2h} \ ^1A_g$	+3.76	+4.65

<sup>a</sup> The labeling of the structures refers to the labels in Figure 1.

were further optimized under their current symmetry at the B3LYP/6-311+G(2d,p) level and frequency calculations were run at the optimized B3LYP/6-311+G(2d,p) geometry. The structures with imaginary frequencies were distorted until structures with real frequencies were obtained. The lower energy isomers from the B3LYP/6-311+G(2d,p) optimization were reoptimized at the CCSD/cc-PVTZ or the CCSD/6-311+G(2d,p) level of theory, running frequency calculations again at this level of theory. Finally, single-point CCSD(T) calculations were run at the CCSD optimized geometries to obtain the total and binding (atomization) energies at a reasonably high level of theory and reasonable computational cost, which allows possible future calculations and comparisons with larger clusters.

It is assumed that this scheme of combining B3LYP and CCSD(T) methods in a plethora of plausible initial geometries followed by unconstrained and constrained geometry optimizations together with vibrational analysis can provide real global (in addition to local) minima of the structures under study. It has been earlier illustrated that the DFT-B3LYP method can provide good results for silicon<sup>25</sup> and hydrogenated silicon<sup>17</sup> and carbon<sup>20,21</sup> clusters and nanocrystals. Good results have been also obtained for  $Si_nC_m$  clusters,<sup>8,11,12</sup> although B3LYP has been criticized for the case of the  $SiC_2$  in comparison to other functionals<sup>33</sup> for which very small energy barriers and energy differences of the order of 1 kcal/mol were involved, causing other high-level methods to fail as well. However, even in this case, as will be illustrated below, the CCSD/CCSD(T) method has produced the correct results. Therefore, the combination of B3LYP and CCSD(T) methods can be considered quite sufficient for these clusters.

## 3. Results and Discussion for $Si_2C_2$ , $Si_2C_2H_2$ , and $C_2B_2H_4$

**3.1.  $Si_2C_2$ .** The lowest energy structures of  $Si_2C_2$  are shown in Figure 1, whereas their total energy and energy differences are summarized in Table 1. As we can see in Table 1, the lowest energy structure is the rhombus in Figure 1, structure 1, characterized by  $D_{2h}$  symmetry. This is true in all levels of

theory except DFT/B3LYP, which favors the triplet linear structure of Figure 1, structure 2, as the lowest energy isomer. This is due to very small energy barrier and an energy difference of 1 kcal/mol, as was shown by multireference calculations by Rintelman and Gordon.<sup>10</sup> This value is barely within the limits of numerical accuracy and is very reminiscent of the case of the  $\text{Si}_6$  cluster, which was shown to be fluxional.<sup>24</sup> Therefore, there should be no surprise that B3LYP fails in this particular case.

As a matter of fact this seems to be the case for  $\text{Si}_2\text{C}_2$  and  $\text{Si}_2\text{C}_2^-$  too. Different multireference calculations (MRCI and multicanonical Monte Carlo simulations) by Bandyopadhyay et al.<sup>9</sup> for the  $\text{Si}_2\text{C}_2^-$  have shown that the experimental photoelectron spectrum of  $\text{Si}_2\text{C}_2^-$  cannot be explained by a single isomer, but a mixture of the “ring” and linear isomers is necessary. Here too, the CCSD(T)/cc-pvtz results give a difference of 0.6 kcal/mol for these structures. Thus, both  $\text{Si}_2\text{C}_2$  and  $\text{Si}_2\text{C}_2^-$  appear to be fluxional.

The “ring structure” in Bandyopadhyay et al.’s<sup>9</sup> work is the distorted rhombus, structure 3 in Figure 1, which for the neutral cluster is very close to, but lower than, the triplet linear state, at the CCSD(T)/6-311+G(2d,p) level. Thus, according to the results of Table 1, the linear structure is actually the third lowest, following the distorted rhombus of Figure 1, structure 3, which is only 0.18 eV (about 4.2 kcal/mol) higher (at the CCSD(T)/6-311+G(2d,p) level) above the rhombic ground state. This value is consistent with the +6 kcal/mol given by the multireference calculations of Rintelman and Gordon<sup>10</sup> for this structure.

As we can see in Figure 1, this structure, compared to the lowest energy rhombus which is characterized by a relatively strong C–C bond and four Si–C bonds, has a slightly stronger C–C bond and an additional Si–Si bond but only three Si–C bonds. The linear state has only two Si–C bonds of relatively higher strength. The linear  $^1\Sigma_g$  spin-singlet state is the fourth lowest state at 0.63 eV above the ground state, whereas the distorted tetragon in Figure 1, structure 4, is next at +1.56 eV. The structure in Figure 1, structure 5, of  $C_s$  near  $C_{2v}$  symmetry comes from a truncated  $T_d$  fragment of silicon (after the replacement by carbon of two silicon atoms), whereas the structure in Figure 1, structure 6, is related to the ground state by “bond-length isomerization”. Both structures are much higher in energy relative to the rest (+1.92 and +4.65 eV, respectively, above the ground state).

Since the focus of the present work is  $\text{Si}_2\text{C}_2\text{H}_2$  and not  $\text{Si}_2\text{C}_2$ , no further results on  $\text{Si}_2\text{C}_2$ , will be presented. However, we should also observe in Table 1 that the B3LYP and CCSD(T) results, with the exception of the triplet linear state, are roughly similar. Also, from the value of atomization energy for the lowest energy rhombic structure and the relative energies, we can see that the atomization energies of the various isomers in Table 1 vary between 11.76 and 8 eV which is quite large.

**3.2.  $\text{Si}_2\text{C}_2\text{H}_2$ . 3.2.1. Structural Properties.** The lower energy isomers of  $\text{Si}_2\text{C}_2\text{H}_2$  are shown in Figure 2. The structures in Figure 2, from a to h, are presented in order of increased energy, except for 2c and 2d, which are shown immediately after the lowest energy structures 2a and 2b due to their closer relationship as will be explained below. Starting from the end, we can recognize isomer 2h as the lowest energy isomer of the form (SiH)SiC(CH) which, however, as we can see in Table 2, is 1.42 eV higher compared to the lowest energy structure. This structure was obtained by Si, C-hydrogenation, and geometry optimization of the  $\text{Si}_2\text{C}_2$  ground-state rhombus. Similarly, isomer 2g is the lowest energy isomer of the form (SiH)-

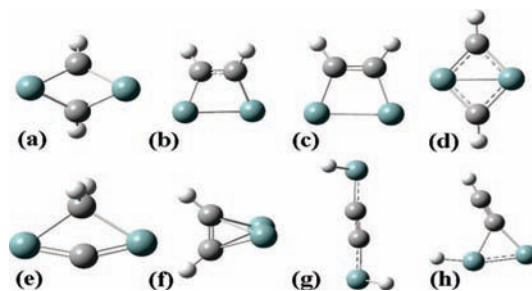


Figure 2. Lower energy structures of  $\text{Si}_2\text{C}_2\text{H}_2$ .

TABLE 2: Relative Energies of  $\text{Si}_2\text{C}_2\text{H}_2$  Structures (in eV), at the B3LYP and CCSD(T) Levels of Theory, Together With B3LYP HOMO–LUMO (H–L) Gaps, Calculated Atomization Energies  $E_b$ , and Atomization Energy Differences ( $\Delta E_b$ ) with Respect to the Corresponding  $\text{Si}_4\text{C}_2$  Clusters<sup>a</sup>

structure/symmetry	B3LYP	CCSDT	$E_b$	$[\Delta E_b]$	H–L
2a $C_{2v}$	+0.32	+0.30	22.93	12.72	4.54
2b $C_2$	0.0	0.0	23.25	13.04	4.12
2c $C_{2v}$	+1.04		22.20	12.00	
2d $C_{2v}$	+0.94	+1.12			2.00
2e $C_{2v}$	+0.77	+0.75	22.46	12.78	3.69
2f $C_s$	+1.06		22.19	12.51	
2g $C_2$	+1.31				
2h $C_s$	+1.42				

<sup>a</sup> The reference energy of structure 2b is  $-656.368482$  (B3LYP) and  $-655.209151$  (CCSD(T)) Hy.

CC(SiH), again quite higher (by 1.31 eV) in energy compared to the ground state. Its small energy gain compared to the isomer 2h seems to come from stronger Si–C bonds. This isomer is obtained by silicon hydrogenation followed by geometry optimization (and reoptimization after distortion according to imaginary frequency modes wherever needed) of both rhombus and linear lowest-lying isomers of  $\text{Si}_2\text{C}_2$ .

The structure in Figure 2f is related to the structure of Figure 1, structure 5, which is the only low-lying three-dimensional isomer of  $\text{Si}_2\text{C}_2$ . Indeed, this structure has been obtained from the structure of Figure 1, structure 5, by attaching two hydrogen atoms on two separate carbons and further optimization, whereas by placing the two hydrogen atoms onto the same carbon atom we obtain the isomer of Figure 2e. This isomer, which is the lowest energy isomer of the form  $(\text{CSi}_2)(\text{CH}_2)$ , is stable with real frequencies, contrary to the structure 2f which has imaginary vibrational frequencies. Distorting the structure 2f according to the imaginary frequency eigenvectors, we are led to the planar structure of Figure 2c, which was originally obtained by hydrogenation of the structure in Figure 1, structure 4. However, structure 2c is also dynamically unstable, with imaginary frequency vibrational modes which tend to destroy planarity. Following the displacement patterns of the imaginary frequency mode(s) we are finally led (after optimization) to the “puckered” ground-state structure of Figure 2b, which is not planar. It has been shown<sup>20,21</sup> that this type of puckering improves the  $\text{sp}^3$  bonding by better optimization of the  $\text{sp}^3$  bond angles.

Before discussing the isomer in Figure 2a, which was placed in front of isomer 2b although higher in energy for “historical” reasons, it is worth discussing briefly isomer 2d which, as we can see in Figure 2, is related to 2a through bond-length isomerization. Isomer 2d was obtained directly from the rhombus of Figure 1, structure 6, not of Figure 1, structure 1, through successive geometry optimizations after distortions according to the eigenvectors of the imaginary frequency modes.

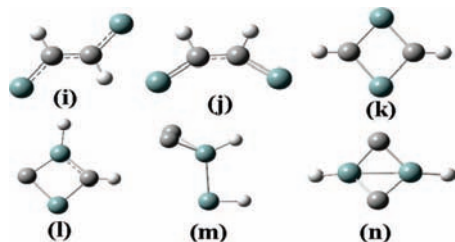


Figure 3. Higher energy structures of  $\text{Si}_2\text{C}_2\text{H}_2$ .

Although the silicon and carbon atoms are in the same plane, the two C–H bonds are bent above and below this plane, respectively.

From the planar counterpart of this isomer (before bending of C–H bonds), following the logic of a diamond–square–diamond (DSD) transformation (with the role of “square” assigned to the planar structure of Figure 2c) we have obtained the structure of Figure 2a. This structure has lower energy than both structures 2d and 2c and real frequencies. The corresponding structure of the isovalent  $\text{C}_2\text{B}_2\text{H}_4$  is the ground state; this is why this structure was placed before the real ground state of Figure 2b, for reasons of direct comparison with  $\text{C}_2\text{B}_2\text{H}_4$ . Thus, we see that the planar structure in Figure 2c is related directly or indirectly with the other three structures in the top row of Figure 2.

Finally, for completeness, the structures of higher (than 1.4 eV) energy are shown in Figure 3.

Both isomers in Figure 3, structures i and j, were obtained by suitable hydrogenation of the linear  $\text{Si}_2\text{C}_2$  structure of Figure 1, structure 2. These isomers were alternatively obtained from the rhombus in Figure 1, structure 1. Structures k, l, and m, were obtained from the structures of Figure 1, structures 4, 5, and 6, respectively. Structure 3n was also obtained from the rhombus of Figure 1, structure 6. Many of these structures have imaginary frequencies at the CCSD and B3LYP levels of theory. It is interesting to note that distortion according to the imaginary frequency modes of these structures finally leads either to the lowest or to the second lowest structure of Figure 2a and 2b, respectively. For structures with two hydrogens on the same carbon atom, the imaginary frequency modes usually lead to the isomer of Figure 2e. Several more structures have been obtained with even higher energies up to 6 eV which are not presented here.

One could also think that through the inverse process of dehydrogenation of  $\text{Si}_2\text{C}_2\text{H}_2$  the lowest energy structures of  $\text{Si}_2\text{C}_2$  could be obtained. This is indeed true.

Finally, as a general rule, we can see that most or all lower energy structures of  $\text{Si}_2\text{C}_2\text{H}_2$  have been obtained from the higher energy structures of  $\text{Si}_2\text{C}_2$ . Apparently the role of hydrogen is more important for the more poorly bonded (lower atomization energy) structures. As we can see in Table 2, the atomization energies of the hydrogenated clusters are larger by almost a factor of 2. We can also observe that in all lower energy structures the hydrogen atoms are attached to carbon atoms, either to separate (ground state and second lowest structure) or to the same carbon atom(s), (for the third lowest structure). This is also true for the other two similar hydrogenated clusters examined here. Therefore, it seems that the stronger C–H interaction compared to Si–H is more important than the (even partial) saturation of the silicon dangling bonds. This is very important for the analogy (homology) to  $\text{C}_2\text{B}_2\text{H}_4$  which is based on the “replacement” of all B–H units by silicons.<sup>24</sup>

**3.2.2. Energetic and Cohesive Properties.** The energetic and cohesive properties of the structures in Figure 2 are shown in

TABLE 3: Relative Energies and Symmetries of the Structures of Figure 3 at the B3LYP Level of Theory

structure/symmetry	i $C_{2h}$	j $C_{2h}$	k $D_{2h}$	l $C_s$	m $C_s$	n $C_s$
$\Delta E$ (eV)	1.43	1.51	1.92	3.65	3.78	4.60

Table 2. For the dynamically unstable (with imaginary frequencies) and the higher energy structures only the B3LYP values are given. The B3LYP and CCSD(T) results for the energy differences are comparable. Therefore, the results and discussion of the atomization energies are restricted to the B3LYP level. As we can see in Table 2, the atomization energies are much higher (by a factor of 2) compared to the plain  $\text{Si}_2\text{C}_2$  clusters, revealing the much higher “stability” of the hydrogenated clusters. The term higher stability reflects mainly the higher atomization energy but is not restricted to just that. The atomization energy differences,  $\Delta E_b$ , besides the difference in stability between these two clusters give also the energy released when the  $\text{Si}_4\text{C}_2\text{H}_2$  cluster breaks into  $\text{Si}_4\text{C}_2$  (at the optimized geometry) and two hydrogen atoms. This energy, about 13 eV, is very large indeed. If we consider instead the stability against  $\text{H}_2$  formation according to the hypothetical reaction  $\text{Si}_2\text{C}_2\text{H}_2 \rightarrow \text{Si}_2\text{C}_2 + \text{H}_2 + \Delta Q$ , we find  $\Delta Q = -8.27$  eV, which is a very high exothermicity for the ground state. In this value, the zero-energy corrections are not included because the emphasis is not on the reaction itself but on the “stability” of these species judged on the basis of various criteria. For the second lowest structure of Figure 2a we find  $\Delta Q = -7.95$  eV.

As an additional criterion of stability one could use the cohesive energy per silicon atom,  $E_{\text{coh}}$ , given by the formula:  $E_{\text{coh}} = [E_b(\text{Si}_n\text{C}_2\text{H}_2) + 2\mu_{\text{H}}]/n$ , where  $E_b(\text{Si}_n\text{C}_2\text{H}_2)$  is the binding (or atomization) energy of the  $\text{Si}_n\text{C}_2\text{H}_2$  cluster and  $\mu_{\text{H}}$  is the chemical potential of H, which is taken at a constant value, with zero corresponding to the value at which the formation energy of methane ( $\text{CH}_4$ ) is zero. The factor of 2 in front of the chemical potential reflects the number of C–H bonds. With the above definition of “cohesive energy” we have effectively removed the energy contribution of all C–H bonds in every cluster and essentially considered the binding energy of the “silicon–carbon skeleton”. This type of definition of cohesive energy is not uncommon.<sup>20</sup> At the B3LYP level the calculated value of  $\mu_{\text{H}}$  is  $-2.58$  eV. Therefore, for the lowest energy structure of  $\text{Si}_2\text{C}_2\text{H}_2$  we find  $E_{\text{coh}} = 9.045$  eV. The corresponding value for  $\text{Si}_2\text{C}_2$  ( $2\mu_{\text{H}} = 0$ ) is 5.88 eV, again almost half the value of  $\text{Si}_2\text{C}_2\text{H}_2$ .

In Table 2 we can also observe that the HOMO–LUMO gaps, which are a zero-order estimate of the chemical rigidity of the clusters, are generally quite high for the lowest energy structures.

Finally, as before, for completeness in Table 3 we give the relative energies of some high-energy structures of Figure 3.

**3.2.3. Bonding Properties.** The bond lengths of the two lowest energy isomers and of some higher energy structures (shown in Figure 2), are given in Table 4. In the same table, the shared electron numbers (SEN) for two-, three-, and four-center bonds are provided using a population analysis based on the method of Roby–Davidson–Heinzmann–Ahlrichs<sup>34–36</sup> (RDHA). Through the RDHA method one can quantify the multicenter bonding, which is a characteristic feature of these species (similar to the isovalent carboranes). As we can see in Table 4 (and Figure 2) the stability of the second lowest energy structure 2a, is characterized by four (instead of two in 2b) relatively strong S–C (SEN = 1.74) bonds, one weak C–C bond, and no Si–Si bonds.

On the other hand the lowest energy structure 2b forms one strong C–C (almost double) bond with length about 1.40 Å

**TABLE 4: Bond Lengths and SEN (for the Two Lowest Energy Structures) of Si<sub>2</sub>C<sub>2</sub>H<sub>2</sub> at the CCSD and B3LYP (in Italics) Levels of Theory<sup>a</sup>**

structure	C–C (Å)	C–Si (Å)	Si–Si (Å)	2-, 3-, and 4-center SEN
2a	<i>(1.688)</i>	<i>1.847</i>	<i>(2.957)</i>	C(1)C(2) 1.14, C(1)Si(3) 1.74, Si(3)Si(4) 0.24,
<i>C<sub>2v</sub></i>	<i>(1.685)</i>	<i>1.857</i>	<i>(2.974)</i>	C(1)C(2) Si(3) 0.43, C(1)Si(3)Si(4) 0.15, C(1)C(2)Si(3)Si(4) 0.12
2b	<i>1.395</i>	<i>1.837</i>	<i>2.416</i>	C(1)C(2) 1.90, C(1)Si(3) 0.59, C(1)Si(4) 1.89
<i>C<sub>2</sub></i>	<i>1.399</i>	<i>1.835</i>	<i>2.413</i>	Si(3)Si(4) 1.41, C(1)C(2)Si(3) 0.28, C(1)Si(3)Si(4) 0.29
2c	1.362	1.920	2.544	
2d	<i>(2.754)</i>	1.810	2.349	
2e	<i>(1.668)</i>	1.739 2.093	<i>(3.371)</i>	

<sup>a</sup> Only SEN values larger than 0.05 are listed. For symmetry equivalent atoms SEN values are not shown.

**TABLE 5: Dominant IR Frequencies and ZPE of the Two Lowest Energy Isomers of Si<sub>2</sub>C<sub>2</sub>H<sub>2</sub> at the CCSD/6-311+(2d,p) Level of Theory<sup>a</sup>**

structure	ZPE (Hy)	freq (cm <sup>-1</sup> )
2a	0.03169	1203 (B <sub>2</sub> ) 100%, 826 (B <sub>2</sub> ) 16%, 336 (A <sub>1</sub> ) 7%
<i>C<sub>2v</sub></i>		304 (B <sub>2</sub> ) 6%, 3126 (A <sub>1</sub> ) 5%, 1508 (A <sub>1</sub> ) 4% 3216 (B <sub>1</sub> ) 2%, 134 (B <sub>1</sub> ) 1%
2b	0.03234	819 (B) 100%, 1233 (B) 32%, 851 (A) 18%
<i>C<sub>2</sub></i>		350 (B) 16%, 790 (B) 13%, 3204 (A) 7% 1302 (A) 5%, 3190 (B) 4%

<sup>a</sup> Frequencies are characterized by symmetry and relative intensity (%). The frequencies and ZPE are unscaled.

and two strong Si–C bonds (bond length, 1.835 Å, and SEN = 1.89) In addition, there are two “half” diagonal Si–C bonds with SEN = 0.59. As a result the amount of multicenter bonding (characterized by three- and four-center SEN) in isomer 2a) is larger compared to isomer 2b. The third lower energy isomer of Figure 2e has two very strong Si–C double bonds (of length about 1.74 Å) and two much weaker Si–C bonds (of about 2.10 Å length) without any C–C or Si–Si bonds This can explain the difference of 0.77 eV from structure 2b. The fourth lower isomer of Figure 2d, like isomer 2a, has no strong C–C bonds but four (stronger) Si–C bonds and an additional Si–Si bond which is not present in isomer 2a. However, the C–C distance in structure 2a is 1.68 Å (a weak bond), compared to 2.75 Å in structure 2d. This seems to be enough to account for the energy difference of about 0.6 eV between these two structures.

**3.2.4. Vibrational Properties.** As was speculated (and anticipated) in the Introduction, Si<sub>2</sub>C<sub>2</sub>H<sub>2</sub> (and perhaps other similar hydrogenated silicon–carbon clusters) could be present in large abundances in interstellar space. Therefore, it is important to examine and compare some characteristic IR frequencies (and intensities) with the corresponding interstellar IR emission data. In Table 5 some “dominant” (relatively high intensity) IR frequencies are presented for the lowest energy isomers, together with the corresponding zero-point energies (ZPE).

From Table 5, we can see that Si<sub>2</sub>C<sub>2</sub>H<sub>2</sub> has IR lines very close to the measured peak value of 1280 and the 3050 cm<sup>-1</sup> value observed at the edge of the stellar IR plateau, which cannot be assigned to any of the known saturated hydrocarbons or fullerenes.<sup>11</sup> The IR line at 1280 cm<sup>-1</sup> is due to a C–H bond-bending mode, whereas the line at 3140 cm<sup>-1</sup> is due to a C–H bond-stretching mode. Furthermore (and more important) as we can see in Table 5, for both isomers the maximum or second maximum IR intensities (1203 and 1233 cm<sup>-1</sup>) are very close to the observed stellar IR peak frequency (within 4%). This is very important, since Webster<sup>19</sup> has used exactly this feature (that the peak intensity corresponds to the 1280 cm<sup>-1</sup> mode) as strong evidence to suggest the existence of C<sub>60</sub>H<sub>60</sub> in stellar atmospheres. Ironically more recent calculations<sup>20</sup> have shown that this is not true for C<sub>60</sub>H<sub>60</sub>. Therefore, this additional feature seems to be highly suggestive that Si<sub>2</sub>C<sub>2</sub>H<sub>2</sub> could be present in interstellar space and stellar atmospheres.

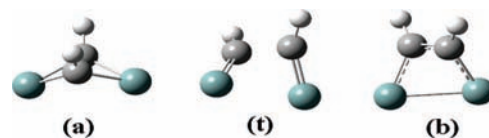


**Figure 4.** “Route” from isomer 1,3- (a) to the 1,2-isomer (b) of Si<sub>2</sub>C<sub>2</sub>H<sub>2</sub> through the transition state (t).

Finally from the values of ZPE we can see that the energy difference between the two lowest energy isomers is practically not affected by the vibrational energy, since the resulting difference is smaller than 0.02 eV.

**3.2.5. Nuclear Rearrangement Properties.** From Figure 2 we can see that, like the corresponding carboranes, the Si<sub>2</sub>C<sub>2</sub>H<sub>2</sub> species are isomerizable, with the structures of Figure 2, parts a and b, constituting the 1,3- and 1,2-conformations, respectively. The two planar transition states in Figure 2, parts c and d, do not connect the two puckered 1,3- and 1,2-isomers directly to each other, although they have an energy difference between themselves of 0.10 eV or 9.6 kJ/mol which can be easily overcome. The direct transition state, is shown in Figure 4, structure 4t, together with a side view of the 1,3- and 1,2-isomers of Figure 2, parts a and b, in Figure 4, parts a and b, respectively. The activation barrier from isomer a to isomer b through the transition state t is 0.63 eV or 60.8 kJ/mol which is just at the limit of the “critical” value of 60 kJ/mol (see ref 24) for isomerization. We can therefore conclude that the Si<sub>2</sub>C<sub>2</sub>H<sub>2</sub> species are isomerizable.<sup>24</sup>

**3.3. Comparison of Si<sub>2</sub>C<sub>2</sub>H<sub>2</sub> and C<sub>2</sub>B<sub>2</sub>H<sub>4</sub>.** One central issue of the present work is the similarity (homology) with the corresponding isovalent carboranes. Therefore, the detail comparison of the structural (and bonding) features of the two species is very important. The “remarkable structures” of C<sub>2</sub>B<sub>2</sub>H<sub>4</sub> have been examined in detail more than 20 years ago by Budzelaar et al.<sup>37</sup> (among others<sup>38,39</sup>). These authors have found that the most stable (CH)<sub>2</sub>(BH)<sub>2</sub> isomer is the puckered 1,3-diboretene (isomer 1 in their work) very similar to the second lowest structure of Si<sub>2</sub>C<sub>2</sub>H<sub>2</sub> in Figure 2a, shown here in Figure 5a. The 1,2-isomer (isomer 3 in their work) was found to be planar similar to the planar Si<sub>2</sub>C<sub>2</sub>H<sub>2</sub> structure in Figure 2c. However, this planar structure of (CH)<sub>2</sub>(BH)<sub>2</sub>, as was found here, has imaginary frequency modes, in full analogy to structure 2c, through which it transforms to its puckered counterpart shown in Figure 5b. The “parent” planar structure of this isomer,

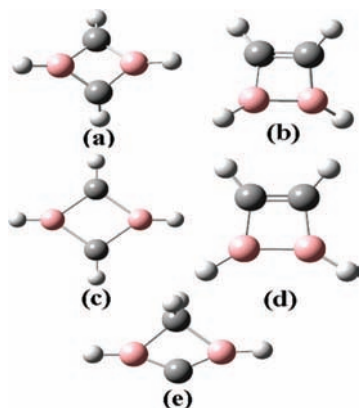


**Figure 5.** Three lower energy structures of  $C_2B_2H_4$ , analogous to structures 1, 3, 11 of Budzelaar et al. (ref 37) in (a), (b), and (e), respectively. Structures c and d are the corresponding planar transition states of structures a and b, respectively.

**TABLE 6: Relative Energies (in eV) of the Structures of  $C_2B_2H_4$  in Figure 5 with Respect to the Lowest Energy Structure at the B3LYP and CCSD(T)/6-311+G(2d,p) Levels of Theory<sup>a</sup>**

structure	method	
	B3LYP	CCSD(T)
	-128.2963852 Hy	-127.9179306Hy
a	0.0	0.0
b	+0.34	+0.34
c	+0.75	
d	+0.72	
e	+0.95	+0.92

<sup>a</sup> The reference energy is listed (in atomic units) in the top row.

which is very similar to the ground-state structure of  $Si_2C_2H_2$ , in Figure 2b, is shown in Figure 5d. According to the calculations of Budzelaar et al.<sup>37</sup> at that time (with the existing computing power), the energy difference between the 1,3-puckered ground-state and the planar isomer in Figure 5d is about 25 kcal/mol (about 1.08 eV) at the MP2/6-31G level, reasonably close (considering the difference in the levels of accuracy) to the value of 0.72 eV found here (see Table 6) at the B3LYP/6-311+G(2d,p). They<sup>37</sup> had not established the dynamical instability of that structure at that time. Instead, they have found a “puckered” transition state (structure 4 in their paper) of  $C_2$  symmetry similar to structure in Figure 5b, about 8 kcal/mol above, through which the planar 1,2-isomer transforms to the puckered 1,3-structure.

This is accomplished, according to Budzelaar et al.,<sup>37</sup> through two successive rotations about the  $C_2$  axis of the BB and CC units with respect to each other. This is allowed in  $C_2$  symmetry and this is what can happen in reality, although the puckered  $C_2$  is not a transition state. Apparently, since the energy difference between the corresponding transition states in Figure 5, parts c and d, is marginal (0.03 eV or 0.7 kcal/mol), this rotation can be easily accomplished through these individual transition states.

Similarly, Budzelaar et al.<sup>37</sup> found that the most stable  $CH_2C(BH)_2$  isomer was a structure (structure 11 in their work) very similar to the  $Si_2C_2H_2$  isomer in Figure 2e. This structure has been also recalculated here and is shown in Figure 5e. Its energy difference from the ground state, as we can see in Table 6, is 0.95 eV at the B3LYP and 0.92 eV at the CCSD(T) level(s) of theory, with the 6-311+G(2d,p) basis. The corresponding  $Si_2C_2H_2$  structure is 0.77 eV above the ground state.

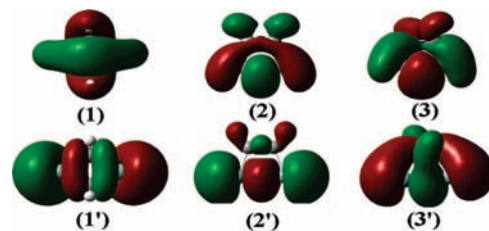


**Figure 6.** HOMO orbitals of the structures in Figure 5, parts a, d, and b, in (1), (2), and (3), respectively, of  $C_2B_2H_4$  (top), together with the corresponding orbitals of  $Si_2C_2H_2$  in Figure 2, parts a, c, and b, respectively (bottom).

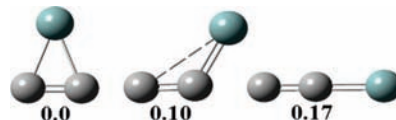


**Figure 7.** Lowest energy structures of  $SiC_2$ . The numerical labels of the structures show their relative CCSD(T)/cc-pvtz energies (in eV).

As we can see by comparison of Figure 5 with Figure 2 (upper part), and of Table 6 with Table 2, the structural similarities between the lowest energy structures of  $Si_2C_2H_2$  and  $C_2B_2H_4$  extend over to energetic similarities except for the reversal in the energy ordering of the 1,2- and 1,3- puckered isomers. In  $Si_2C_2H_2$  the 1,2-isomer instead of the 1,3- is the lowest energy structure. However, looking at the planar 1,3- and 1,2-structures in Figure 5, parts c and d, respectively, we can see from Table 6 that the planar 1,2-structure is lower (by 0.03 eV) from the corresponding planar 1,3 structure. The reversal in energetic ordering between planar and puckered structures is also true for  $Si_2C_2H_2$ . Thus, for both species, the energetic ordering of the puckered 1,2- and 1,3-isomers is reversed from the ordering of the corresponding planar transition states. As a result the energy differences of the puckered isomers of  $Si_2C_2H_2$  are similar to the energy differences of the planar structures of  $C_2B_2H_4$  and vice versa. This is apparently due to the different magnitude of the effect of puckering (which improves the bond angles of the  $sp^3$  bonding) in the two species. The different magnitude of the  $sp^3$  bonding (and the resulting energetic reversal) should be largely responsible for the differences in the HOMO orbitals of the two species in Figure 6, which are otherwise overall similar.

The similarity extends (even stronger) to the rest of the isomers (and transition states) in Figures 2, 3, and 5. For example, the third isomer in Figure 5e, is fully analogous to the isomer of Figure 2e. In addition (from the SEN values in Table 4) we can see that multicenter bonding is very important for both species, and (from the discussion of section 3.2.5) we can also recognize that both systems ( $C_2B_2H_4$  and  $Si_2C_2H_2$ ) are isomerizable.

#### 4. Synopsis of Results for $SiC_2$ , $SiC_2H_2$ , and $C_2BH_3$

**4.1.  $SiC_2$ .** Silicon dicarbide,  $SiC_2$ , is a well-known molecule which is known to exist in interstellar space and stellar atmospheres,<sup>1,2,40</sup> characterized as “astromolecule of the month” February 2005.<sup>40</sup> The here (re)calculated lowest energy structures of this molecule at the CCSD(T)/cc-pvtz level are shown in Figure 7, which shows also their energetic ordering (energy differences).

The structure in the middle (0.10 eV above the lowest energy state) is the lowest energy state at the B3LYP level, whereas at the CCSD(T)/cc-pvtz level it is a transition state.

**4.2.  $SiC_2H_2$ .** The low-energy (up to about 5 eV) isomers of  $SiC_2H_2$  obtained from the structures of  $SiC_2$  are shown in Figure

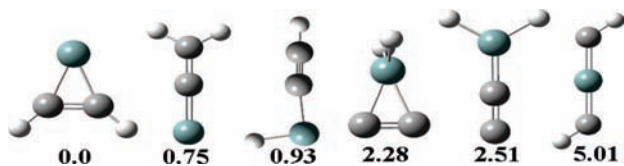


**Figure 8.** Lowest energy isomers of  $\text{SiC}_2\text{H}_2$ . The numerical labels of the structures show their relative CCSD(T)/cc-pvtz energies (in eV).

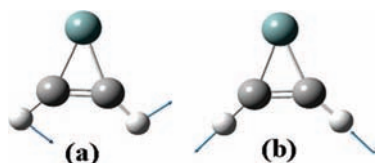


**Figure 9.** Bond-bending (a) and bond-stretching (b) vibrational modes of  $\text{SiC}_2\text{H}_2$ .

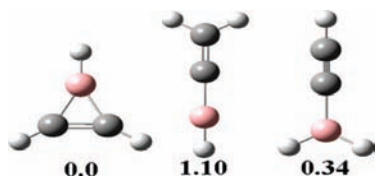


**Figure 10.** Lowest energy isomers of  $\text{C}_2\text{BH}_3$ . The numerical labels of the structures show their relative CCSD(T)/cc-pvtz energies (in eV), according to Krogh-Jespersen et al. (ref 39).

8, which also shows their energetic ordering. All structures are real minima, without imaginary frequencies.

As we can see in Figure 8 the lowest energy isomer is a planar triangular structure with the hydrogens attached (as in  $\text{Si}_2\text{C}_2\text{H}_2$ ) to the two carbon atoms. As in  $\text{Si}_2\text{C}_2\text{H}_2$ , structures with hydrogens attached to the same carbon atom are next in energetic preference, followed by structures with hydrogens in one carbon and one silicon atom. Finally, structures with hydrogens only on silicon atom(s) are energetically higher.

Similarly to  $\text{Si}_2\text{C}_2\text{H}_2$ ,  $\text{SiC}_2\text{H}_2$  also has IR lines in the region of interest (near 1200 and around 3100  $\text{cm}^{-1}$ ). In Figure 9 the C–H bond-bending and bond-stretching modes are shown in Figure 9, parts a and b, respectively, obtained at the CCSD/cc-pvtz level of theory without any scaling. The bond-bending mode in Figure 9a occurs at 1137  $\text{cm}^{-1}$  with intensity 74% of the peak value, whereas the bond-stretching mode at 3208  $\text{cm}^{-1}$  corresponds to only 10% of the peak intensity. Both modes are characterized by  $B_2$  symmetry.

**4.3. Comparison of  $\text{C}_2\text{BH}_3$  and  $\text{SiC}_2\text{H}_2$ .** The three-member  $\text{C}_2\text{BH}_3$  rings have been examined by Krogh-Jespersen et al.<sup>39</sup> earlier and relatively more recently by Galland et al.<sup>41</sup> at various levels of theory (B3LYP, QCSD(T), and CCSD(T)). At all levels of theory the lowest energy structure, known as borirene, is the planar aromatic three-member ring, shown in Figure 10 (0.0), fully analogous to the  $\text{SiC}_2\text{H}_2$  ring in Figure 8 (0.0). We can immediately notice that the three lowest energy isomers of  $\text{C}_2\text{BH}_3$  in Figure 10, known from left to right as borirene, borallene, and ethynylborane, are fully analogous to the first three isomers of  $\text{SiC}_2\text{H}_2$  (from left to right, respectively) in Figure 8. As we can see in Figure 10, the energetic ordering of the second and third isomer has been reversed in comparison to the homologous structures of  $\text{SiC}_2\text{H}_2$  for similar reasons (relative magnitude of  $\text{sp}^3$  bonding) as in  $\text{Si}_2\text{C}_2\text{H}_2$ . As we have seen earlier, the  $\text{sp}^3$  bonding (bond angle) optimization leads to puckering of the bonds in  $\text{Si}_2\text{C}_2\text{H}_2$ , in analogy to bending in the structure of Figure 8 (0.93).

The structural and bonding similarity between  $\text{SiC}_2\text{H}_2$  and  $\text{Si}_2\text{C}_2\text{H}_2$  and the corresponding  $\text{C}_2\text{BH}_3$  and  $\text{C}_2\text{B}_2\text{H}_5$  species is

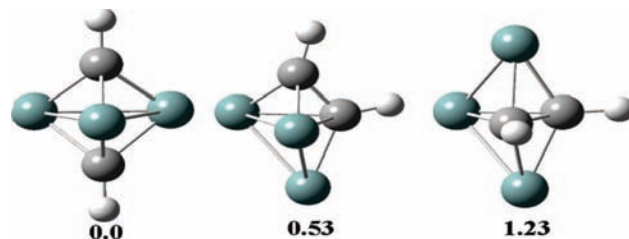


**Figure 11.** Lowest energy isomers of  $\text{Si}_3\text{C}_2\text{H}_2$ . The numerical labels of the structures show their relative CCSD(T)/cc-pvtz energies (in eV).

also stressed by the amount of multicenter (three-center in this limiting case) bonding. The corresponding (1, 2, 3) SEN are practically the same: 0.62 for  $\text{C}_2\text{BH}_3$  and 0.60 for  $\text{SiC}_2\text{H}_2$ .

Furthermore the aromatic properties of the two species are pretty much similar. The nucleus-independent chemical shifts (NICS), evaluated at the ring's center, NICS(0), are a simple and common measure (index) of aromaticity. The NICS(0) value of  $\text{C}_2\text{BH}_3$  is  $-20.4$  ppm at the B3LYP/6-311+G(2d,p) level of theory. The corresponding NICS(0) value for  $\text{SiC}_2\text{H}_2$  is  $-10.7$  ppm. The two negative NICS(0) values reveal a clear aromatic behavior for both species. Thus, in addition to structural, energetic, bonding, and nuclear rearrangement similarity, the two species are characterized also by aromatic similarity (of different magnitude).

## 5. Outline of Results for $\text{Si}_3\text{C}_2\text{H}_2$ and $\text{C}_2\text{B}_3\text{H}_5$

The three lowest energy isomers of  $\text{Si}_3\text{C}_2\text{H}_2$  are shown in order of increase energy in Figure 11. These structures were obtained by hydrogenation of the structures of  $\text{Si}_3\text{C}_2$  obtained from the literature<sup>5a</sup> and/or generated here as was explained in section 2. The lowest energy isomer 11 (0.0) is also the most symmetric one, characterized by  $D_{3h}$  symmetry. This isomer should be considered as obtained from the corresponding  $D_{3h}$  symmetric  $\text{Si}_5^{2-}$  dianion<sup>25</sup> by 1,5-substitution of two Si atoms (lying on a  $C_3$  axis) by C–H units. Similarly the second lowest energy isomer in Figure 11 (0.53) can be obtained from a 1,2-similar substitution. Finally the third isomer in Figure 11 (1.23) is obtained by a 2,3-substitution from  $\text{Si}_5^{2-}$ .

Thus, the stability of the  $\text{Si}_3\text{C}_2\text{H}_2$  isomers, as we can see in Figure 11, is in the following order 1,5- > 1,2- > 2,3-, exactly as the three lowest energy isomers of  $\text{C}_2\text{B}_3\text{H}_5$  (see ref 42). This energetic ordering is in full agreement with known empirical valence rules<sup>42</sup> and topological charge stabilization<sup>28,43</sup> concepts, developed originally for the isovalent carboranes. The 1,5-, 1,2-, and 2,3-carboranes are obtained in a similar fashion from the  $\text{B}_5\text{H}_5^{2-}$  borane, which is isovalent and fully homologous to the  $\text{Si}_5^{2-}$  dianion.<sup>25</sup> As we can see in this case the homology is more complete, without any reversal in energetic ordering. Apparently, this could be attributed to an effective reduction of the  $\text{sp}^3$  in relation to multicenter bonding in view of a larger number of (silicon) atoms. In this respect  $\text{SiC}_2\text{H}_2$ , and in part  $\text{Si}_2\text{C}_2\text{H}_2$ , could be considered as “borderline” cases. Obviously, this and other points raised here need further investigation.

## 6. Conclusions

It has been demonstrated that  $\text{Si}_2\text{C}_2\text{H}_2$  is very stable (more stable than the corresponding  $\text{Si}_2\text{C}_2$  cluster), as is exemplified by the calculated atomization and cohesive energy. The most stable  $\text{Si}_2\text{C}_2\text{H}_2$  isomers arise from the least stable  $\text{Si}_2\text{C}_2$  structures by incorporating hydrogen preferably in two separate (highest stability) or on the same carbon atom. It is very probable

(based on the calculated IR spectrum) that this cluster could exist in interstellar space (cosmic dust) and carbon-rich stars.

Furthermore, it has been shown that  $\text{Si}_2\text{C}_2\text{H}_2$  is fully analogous and homologous to the  $\text{C}_2\text{B}_2\text{H}_4$  carborane and is isomerizable as well. The lowest energy isomers of  $\text{Si}_2\text{C}_2\text{H}_2$  are structurally and electronically similar to lowest energy isomers of  $\text{C}_2\text{B}_2\text{H}_4$ . This is also true for  $\text{SiC}_2\text{H}_2\text{--C}_2\text{BH}_3$  and  $\text{Si}_3\text{C}_2\text{H}_2\text{--C}_2\text{B}_3\text{H}_5$ . The energetic ordering, however, of the two lowest energy isomers in  $\text{Si}_2\text{C}_2\text{H}_2\text{--C}_2\text{B}_2\text{H}_4$  and the second lowest isomers in  $\text{SiC}_2\text{H}_2\text{--C}_2\text{BH}_3$  has been reversed. This is attributed to the different impact of puckering or bending (through which the  $\text{sp}^3$  bond angles tend to be optimized) in these two species. However, in the case of  $\text{Si}_3\text{C}_2\text{H}_2\text{--C}_2\text{B}_3\text{H}_5$  there is a one-to-one correspondence of the three lowest energy structures including also the energetic ordering which is in full agreement with well-known stability rules and criteria.<sup>28,42,43</sup>

These results are indicative and highly suggestive of a more general relationship between clusters of the form  $\text{Si}_{n-2}\text{C}_2\text{H}_2$  and closo-carboranes of the general form  $\text{C}_2\text{B}_{n-2}\text{H}_n$ . It is expected that the present work, with the analogies and similarities revealed, would be very useful for the development and design of novel composite materials and structures based on silicon–carbon. More work is needed in this direction.

## References and Notes

- (1) Michalopoulos, D. L.; Geusic, M. E.; Langridge-Smith, P. R. R.; Smalley, R. E. *J. Chem. Phys.* **1984**, *80*, 3556.
- (2) (a) Trucks, G. W.; Bartlett, R. J. *J. Mol. Struct. (THEOCHEM)* **1986**, *135*, 423. (b) Fitzgerald, G. B.; Bartlett, R. J. *Int. J. Quantum Chem.* **1990**, *38*, 121.
- (3) (a) Mühlhäuser, M.; Froudakis, G. E.; Zdetsis, A. D.; Peyerimhoff, S. D. *Chem. Phys. Lett.* **1993**, *204*, 617. (b) Mühlhäuser, M.; Froudakis, G. E.; Zdetsis, A. D.; Engels, B.; Flytzanis, N.; Peyerimhoff, S. D. *Z. Phys. D: At., Mol. Clusters* **1994**, *32*, 113.
- (4) Rittby, C. M. L. *J. Chem. Phys.* **1994**, *100*, 175.
- (5) (a) Froudakis, G. E.; Mühlhäuser, M.; Zdetsis, A. D. *Chem. Phys. Lett.* **1995**, *233*, 619. (b) Zdetsis, A. D.; Froudakis, G. E.; Mühlhäuser, M.; Thümmel, H. *J. Chem. Phys.* **1996**, *104*, 2566.
- (6) Presilla-Marquez, J. D.; Rittby, C. M. L.; Graham, W. R. M. *J. Chem. Phys.* **1996**, *104*, 2818.
- (7) Hunsicker, S.; Jones, R. O. *J. Chem. Phys.* **1996**, *105*, 5048.
- (8) Bertolus, M.; Brenner, V.; Millié, P. *Eur. Phys. J. D* **1998**, *1*, 197.
- (9) Bandyopadhyay, P.; Ten-no, S.; Iwata, S. *J. Phys. Chem. A* **1999**, *103*, 6442.
- (10) Rintelman, J. M.; Gordon, S. *J. Chem. Phys.* **2001**, *115*, 1795.
- (11) Bertolus, M.; Finocchini, F.; Millié, P. *J. Chem. Phys.* **2004**, *120*, 4333.
- (12) (a) Pradhan, P.; Ray, A. K. *Eur. Phys. J. D* **2006**, *37*, 393. (b) Pradhan, P.; Ray, A. K. *J. Mol. Struct. (THEOCHEM)* **2005**, *716*, 109.
- (13) Hackwell, J. A. *Astron. Astrophys.* **1972**, *21*, 239.
- (14) Cernicharo, J.; Gottlieb, C. A.; Guelin, M.; Thaddeus, P.; Vrtilek, J. M. *Astrophys. J.* **1989**, *341*, L25.
- (15) Rechtsteiner, G. A.; Hampe, O.; Jarrold, M. F. *J. Phys. Chem. B* **2001**, *105*, 4188.
- (16) Karttunen, A. J.; Linnolahti, M.; Pakkanen, T. A. *J. Phys. Chem. C* **2007**, *111*, 2545.
- (17) Zdetsis, A. D. *Phys. Rev. B* **2007**, *76*, 075402.
- (18) Ambrosone, G.; Coscia, U.; Ferrero, S.; Giorgis, F.; Mandracci, P.; Pirri, C. F. *Philos. Mag. B* **2002**, *82*, 35.
- (19) (a) Webster, A. *Nature* **1991**, *352*, 412. (b) Webster, A. *Mon. Not. R. Astron. Soc.* **1992**, *257*, 463.
- (20) Zdetsis, A. D. *Phys. Rev. B* **2008**, *77*, 115402.
- (21) Linnolahti, M.; Karttunen, A. J.; Pakkanen, T. A. *ChemPhysChem* **2006**, *7*, 1661.
- (22) Stoldt, C. R.; Maboudian, R.; Carraro, C. *Astrophys. J.* **2001**, *548*, L225.
- (23) van Diedenhoven, B.; Peeters, E.; van Kerckhoven, C.; Hony, S.; Hudgins, D. M.; Allamandola, L. J.; Tielens, G. G. M. *Astrophys. J.* **2004**, *611*, 928.
- (24) Zdetsis, A. D. *J. Chem. Phys.* **2007**, *127*, 014314.
- (25) Zdetsis, A. D. *J. Chem. Phys.* **2007**, *127*, 244308.
- (26) Lipscomb, W. N. *Science* **1966**, *153*, 373.
- (27) Fox, M. A.; Wade, K. *Pure Appl. Chem.* **2003**, *75*, 1315.
- (28) Williams, R. E. *Chem. Rev.* **1992**, *92*, 177.
- (29) McKee, M. L. In *Encyclopedia of Computational Chemistry*; John Wiley & Sons: New York, 1998; Vol. 2, pp 1002–1013.
- (30) King, R. B. *Chem. Rev.* **2001**, *101*, 1119.
- (31) Stephens, P. J.; Devlin, F. J.; Chabalowski, C. F.; Frisch, M. J. *J. Phys. Chem.* **1994**, *98*, 11623.
- (32) Frisch, M. J.; Trucks, G. W.; Schlegel, H. B.; Scuseria, G. E.; Robb, M. A.; Cheeseman, J. R.; Montgomery, J. A., Jr.; Vreven, T.; Kudin, K. N.; Burant, J. C.; Millam, J. M.; Iyengar, S. S.; Tomasi, J.; Barone, V.; Mennucci, B.; Cossi, M.; Scalmani, G.; Rega, N.; Petersson, G. A.; Nakatsuji, H.; Hada, M.; Ehara, M.; Toyota, K.; Fukuda, R.; Hasegawa, J.; Ishida, M.; Nakajima, T.; Honda, Y.; Kitao, O.; Nakai, H.; Klene, M.; Li, X.; Knox, J. E.; Hratchian, H. P.; Cross, J. B.; Adamo, C.; Jaramillo, J.; Gomperts, R.; Stratmann, R. E.; Yazyev, O.; Austin, A. J.; Cammi, R.; Pomelli, C.; Ochterski, J. W.; Ayala, P. Y.; Morokuma, K.; Voth, G. A.; Salvador, P.; Dannenberg, J. J.; Zakrzewski, V. G.; Dapprich, S.; Daniels, A. D.; Strain, M. C.; Farkas, O.; Malick, D. K.; Rabuck, A. D.; Raghavachari, K.; Foresman, J. B.; Ortiz, J. V.; Cui, Q.; Baboul, A. G.; Clifford, S.; Cioslowski, J.; Stefanov, B. B.; Liu, G.; Liashenko, A.; Piskorz, P.; Komaromi, I.; Martin, R. L.; Fox, D. J.; Keith, T.; Al-Laham, M. A.; Peng, C. Y.; Nanayakkara, A.; Hallacomb, M. C.; Gill, P. M. W.; Johnson, B.; Chen, W.; Wong, M. W.; Gonzalez, C.; Pople, J. A. *Gaussian 03*, revision C.02; Gaussian, Inc.: Pittsburgh, PA, 2004.
- (33) Arulmozhiraja, S.; Kolandaivel, P.; Ohashi, O. *J. Phys. Chem. A* **1999**, *103*, 3073.
- (34) Roby, K. R. *Mol. Phys.* **1974**, *27*, 81.
- (35) Davidson, E. R. *J. Chem. Phys.* **1967**, *46*, 3320.
- (36) Heinzmann, R.; Ahhichs, R. *Theor. Chim. Acta* **1976**, *42*, 33.
- (37) Budzelaar, P. H. M.; Krogh-Jepsen, K.; Clark, T.; Schleyer, P. v. R. *J. Am. Chem. Soc.* **1985**, *107*, 2773.
- (38) Siebert, W. *Pure Appl. Chem.* **1997**, *59*, 947.
- (39) Krogh-Jepsen, K.; Cremer, D.; Dill, J. D.; Pople, J. A.; Schleyer, P. v. R. *J. Am. Chem. Soc.* **1981**, *103*, 2589.
- (40) See, for instance: The Astrochymist. Astromolecule of the Month: <http://www.molres.org/astrochymist/AMOTM/> (accessed Feb 2005).
- (41) Galland, N.; Hannachi, Y.; Lanzisera, D. V.; Andrews, L. *Chem. Phys.* **1998**, *230*, 143.
- (42) Ott, J. J.; Gimarc, B. M. *J. Am. Chem. Soc.* **1986**, *108*, 4303.
- (43) (a) Williams, R. E.; Gerhart, F. J. *J. Am. Chem. Soc.* **1965**, *87*, 3513. (b) Williams, R. E. In *Advances in Organometallic Chemistry*; Stone, F. G., West, R., Eds.; Academic Press: New York, 1994; Vol. 36, pp 1–56.